

Superresolution optical fluctuation imaging (SOFI) & Colocalization case studies

Omar Ramirez Gonzalez

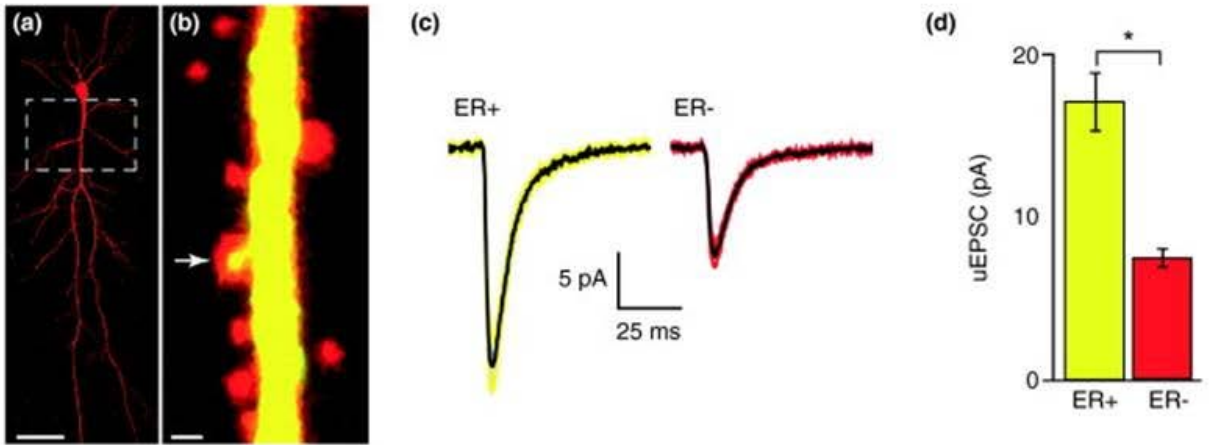
Laboratory for Scientific Image Analysis (SCIAN-Lab), BNI, Program of Anatomy and Development, ICBM, School of Medicine, Universidad de Chile, Santiago, Chile.

07.11.2014

Section 1

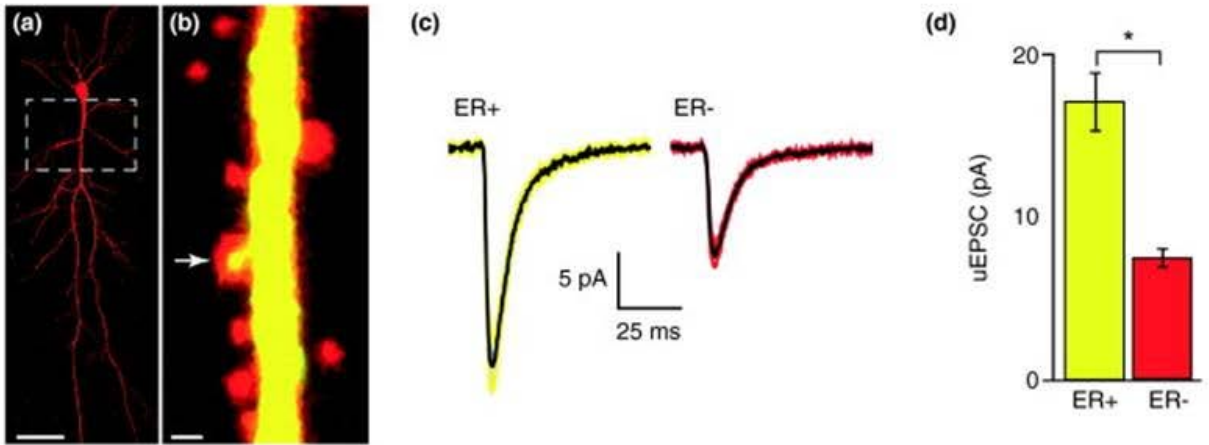
Superresolution optical fluctuation imaging (SOFI)

**A problem in biology: The neuronal ER participates in synaptic potentiation,
How to look at it?**



Holbro *et al.*, PNAS, 2009

**A problem in biology: The neuronal ER participates in synaptic potentiation,
How to look at it?**

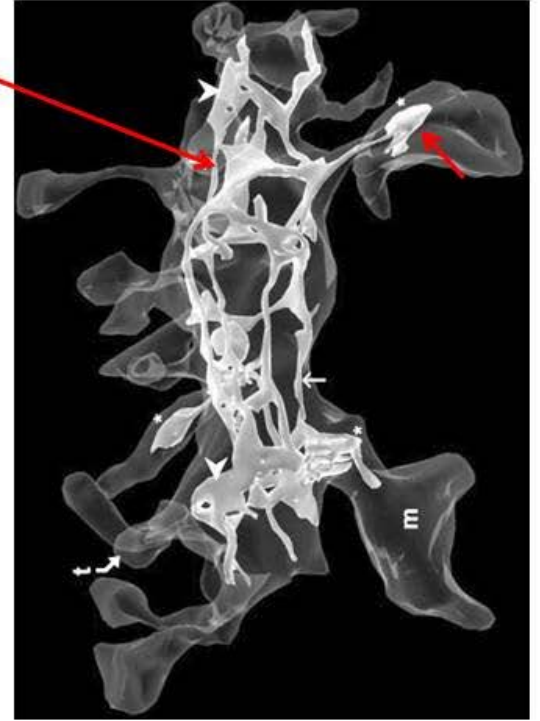
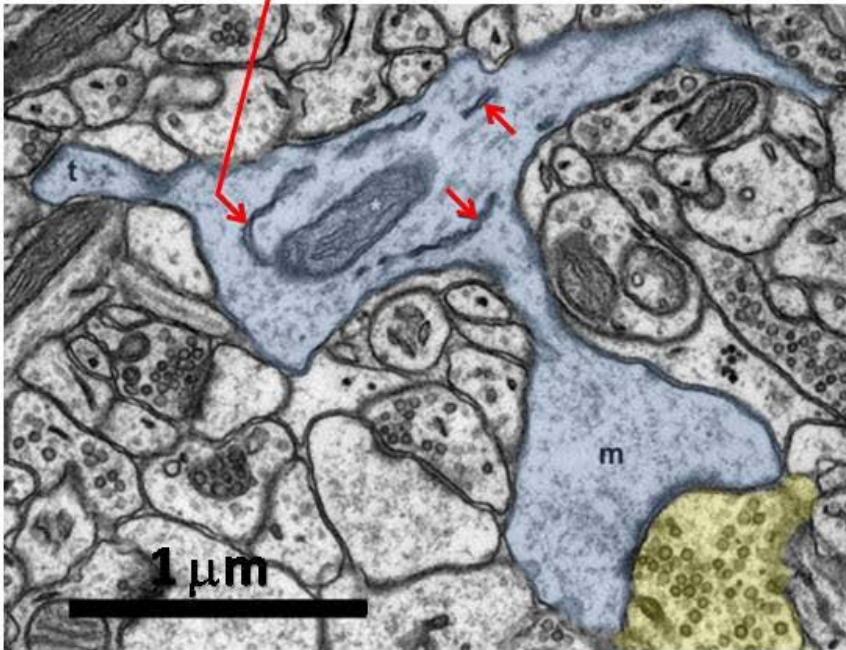


- Neurotransmitter receptor synthesis and transport
- Calcium storage/release

Holbro *et al.*, PNAS, 2009

The neuronal ER is a subdiffraction sized structure

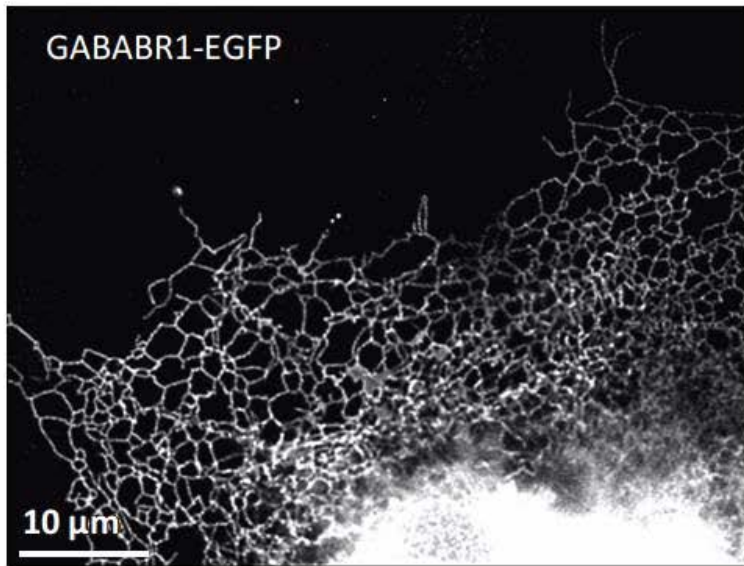
The ER tubule diameter is < 40 nm, far below the ~ 250 nm resolution of conventional optical microscopes.



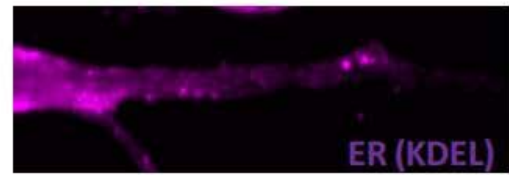
Cooney *et al.*, *J Neuroscience*, 2002

The neuronal ER is a subdiffraction sized structure

COS-7 cells

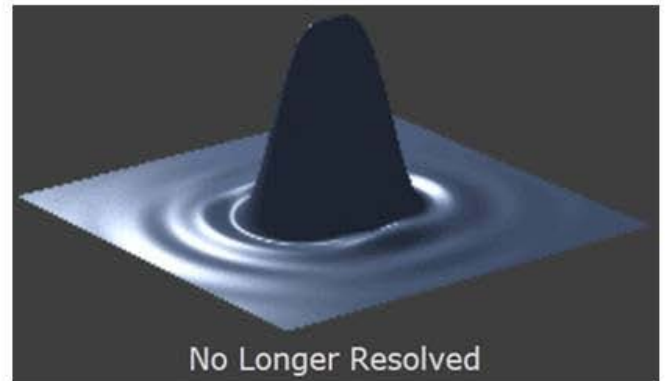
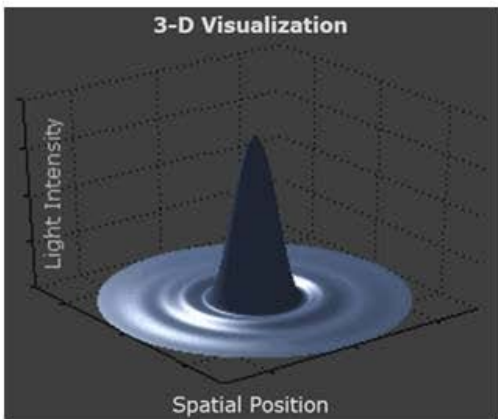
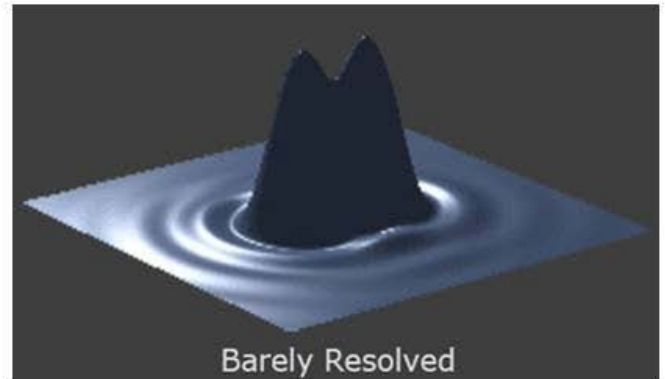
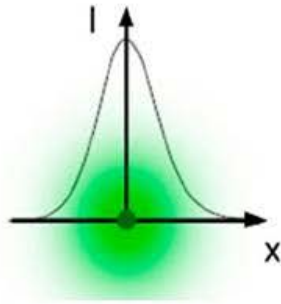
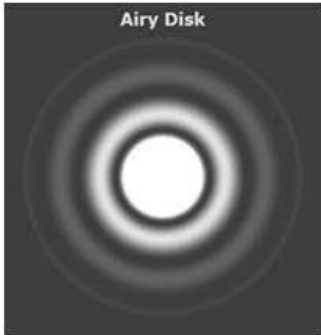


Primary hippocampal neurons







Light diffraction determines and limits resolution

Abbe's formula: $\Delta_{\min} = \frac{\lambda}{2NA}$

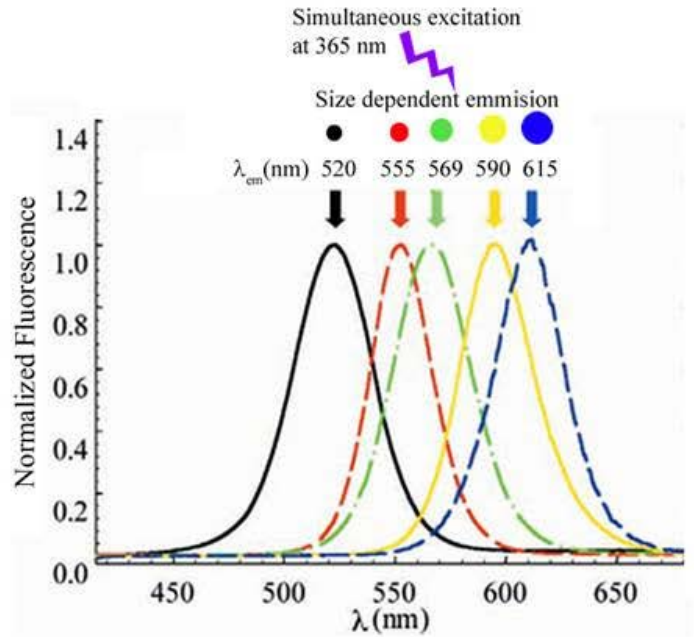
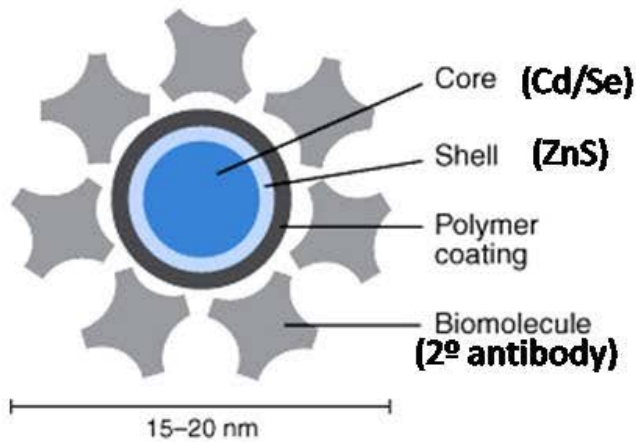


Current superresolution techniques

Technique	Confocal	SIM	STED	PALM
Resolution limit	~250 nm	~120 nm	~60 nm	~30 nm
PSF				
Advantages	Broadly available	Multicolor Flexible labeling Live cell	Two color Single scan imaging Live cell	Multicolor Single molecule tracking
Drawbacks	Diffraction limited ($\lambda/2$)	Resolution limited to ($\lambda/4$) Sensitive to alignment	Limited dye availability Sensitive to alignment Expensive	No endogenous labeling

Superresolution optical fluctuation imaging (SOFI) method

We need a fluctuating light source:
Quantum dots



Joerg Enderlein

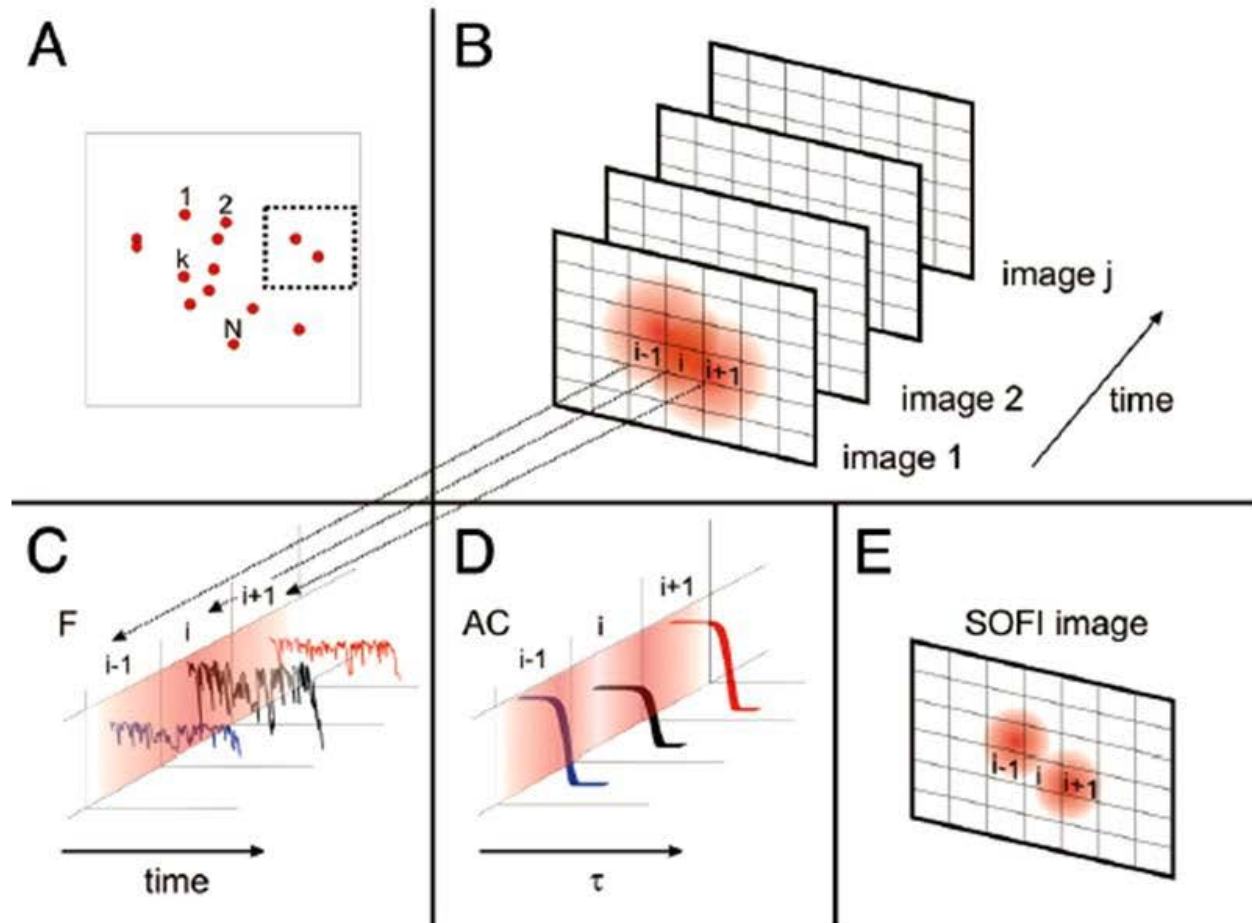
Superresolution optical fluctuation imaging (SOFI) method

ON/OFF fluctuation



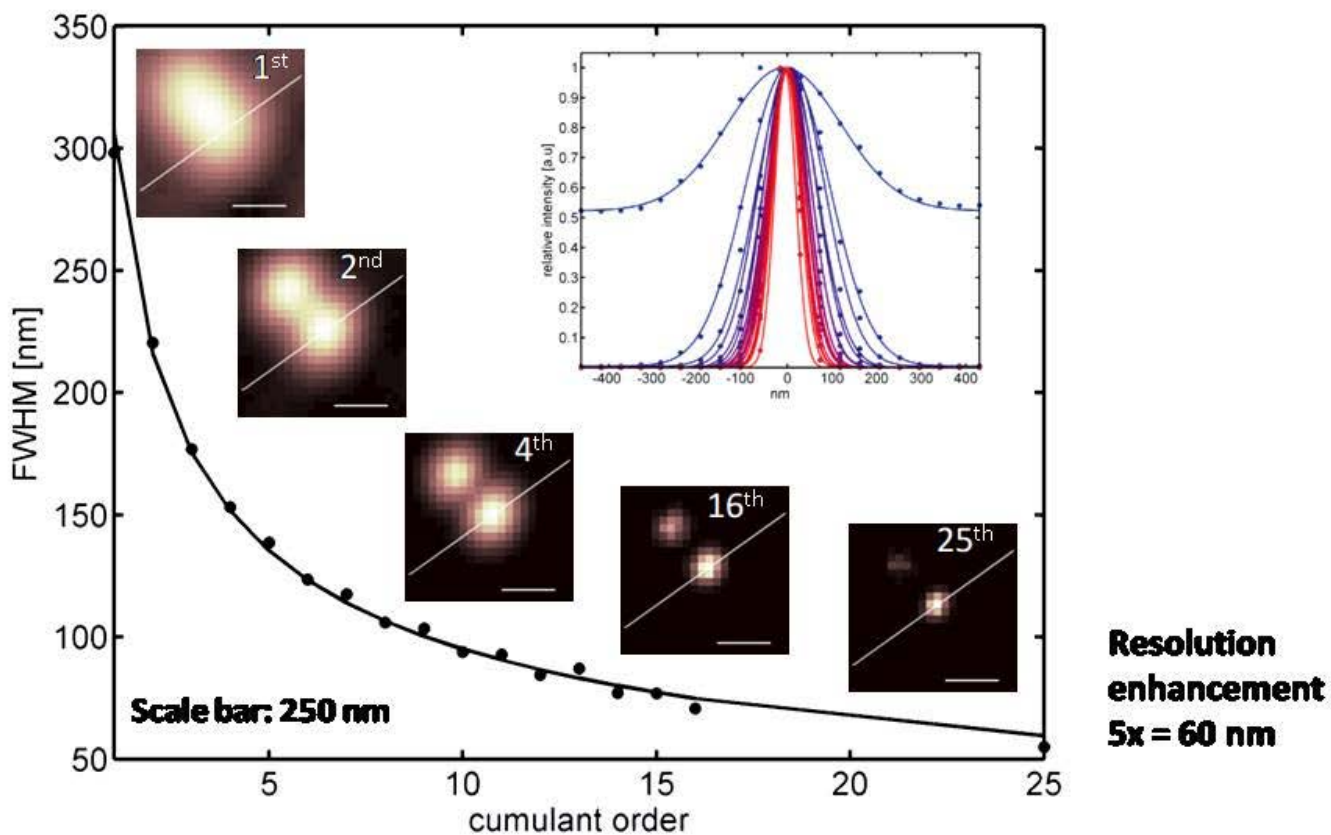
Qdot 625 nm emission wavelength, wide-field microscope,
10 Hz movie with a CCD camera

Image formation with SOFI



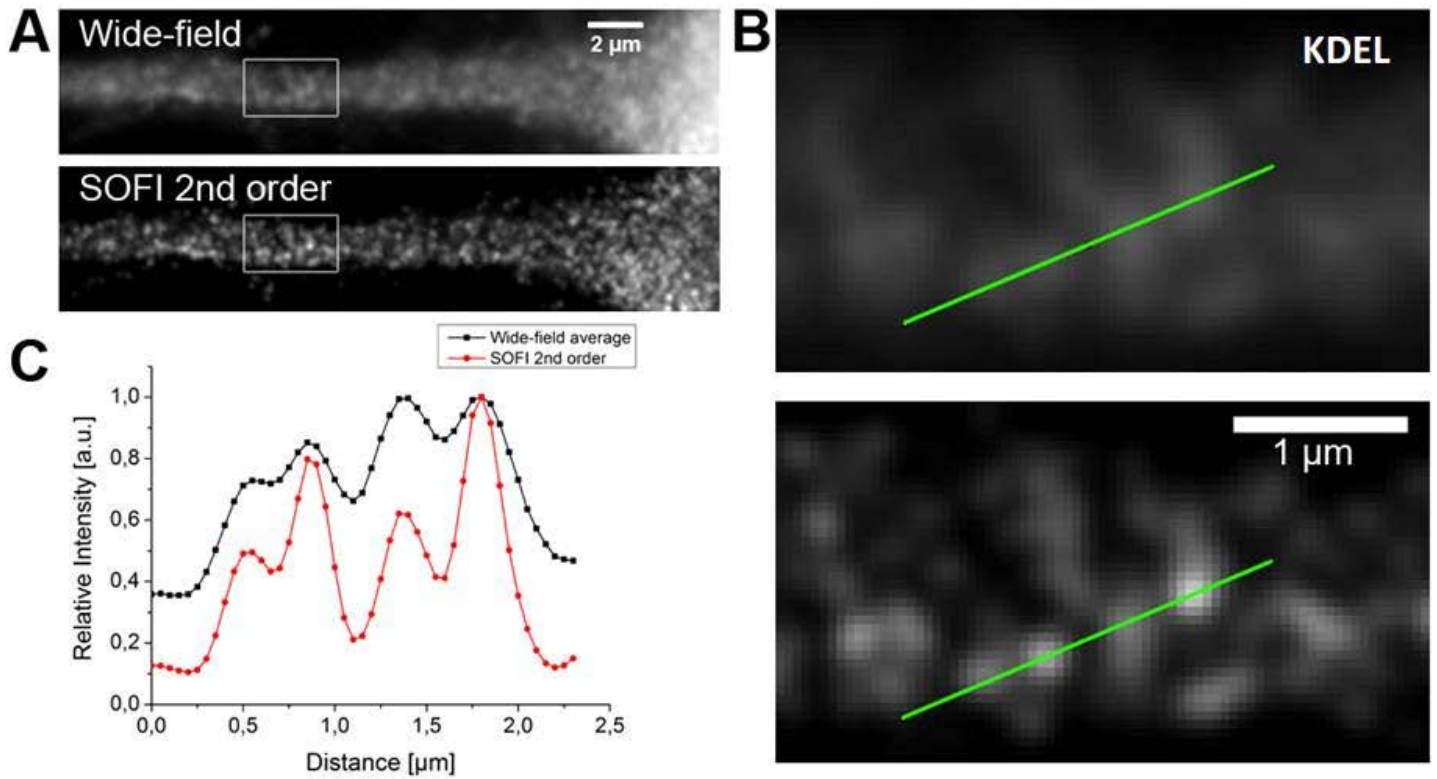
Dertinger T., Colyer R.; Iyer G.; Weiss. S.; Enderlein J., PNAS, 2009

SOFI higher order cumulants

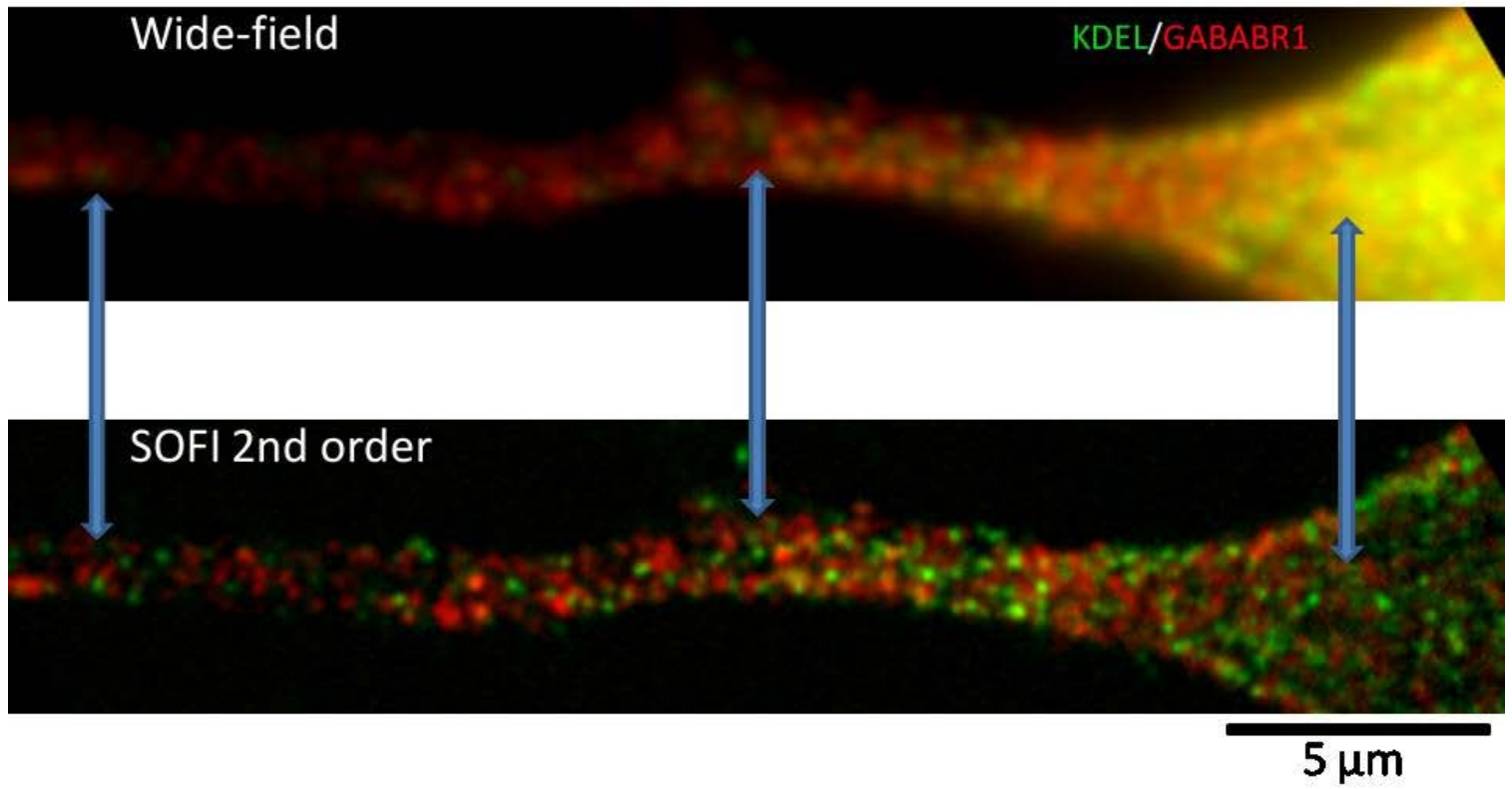


Dertinger T., Colyer R.; Iyer G.; Weiss. S.; Enderlein J., PNAS, 2009

2nd order SOFI applied to a neuronal ER image



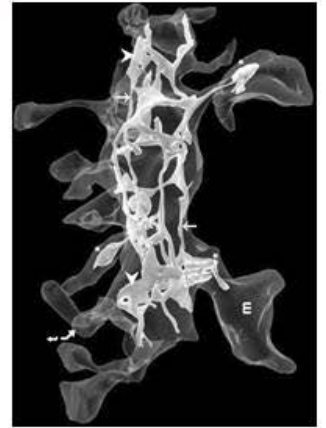
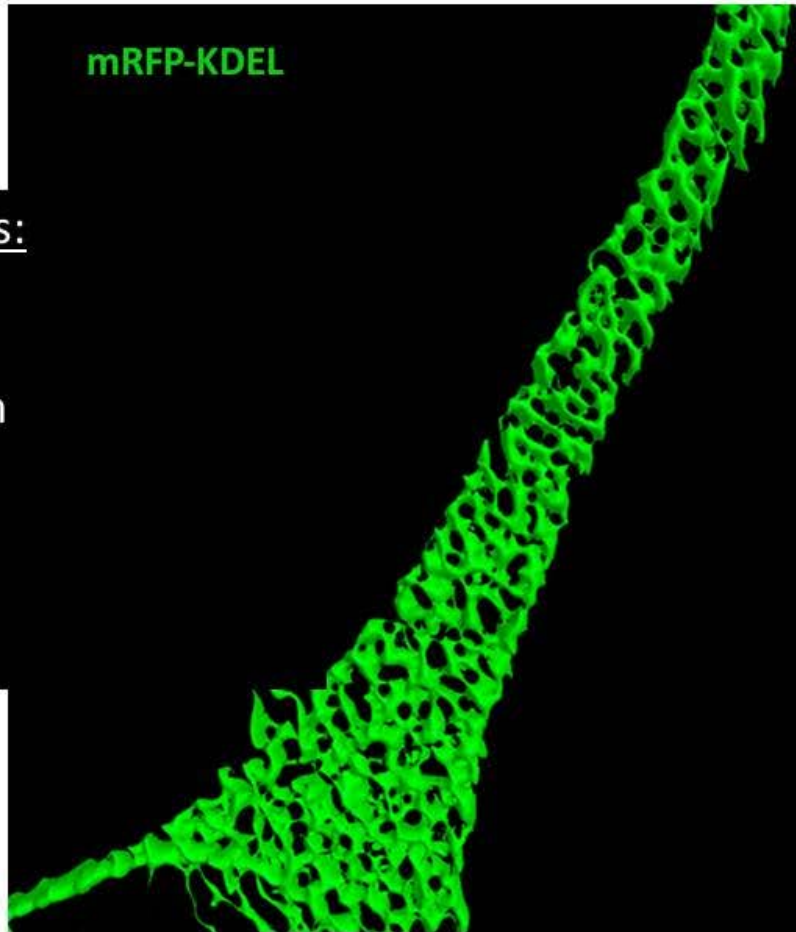
Two channel 2nd order SOFI



2nd order SOFI endoplasmic reticulum 3D reconstruction

SOFI advantages:

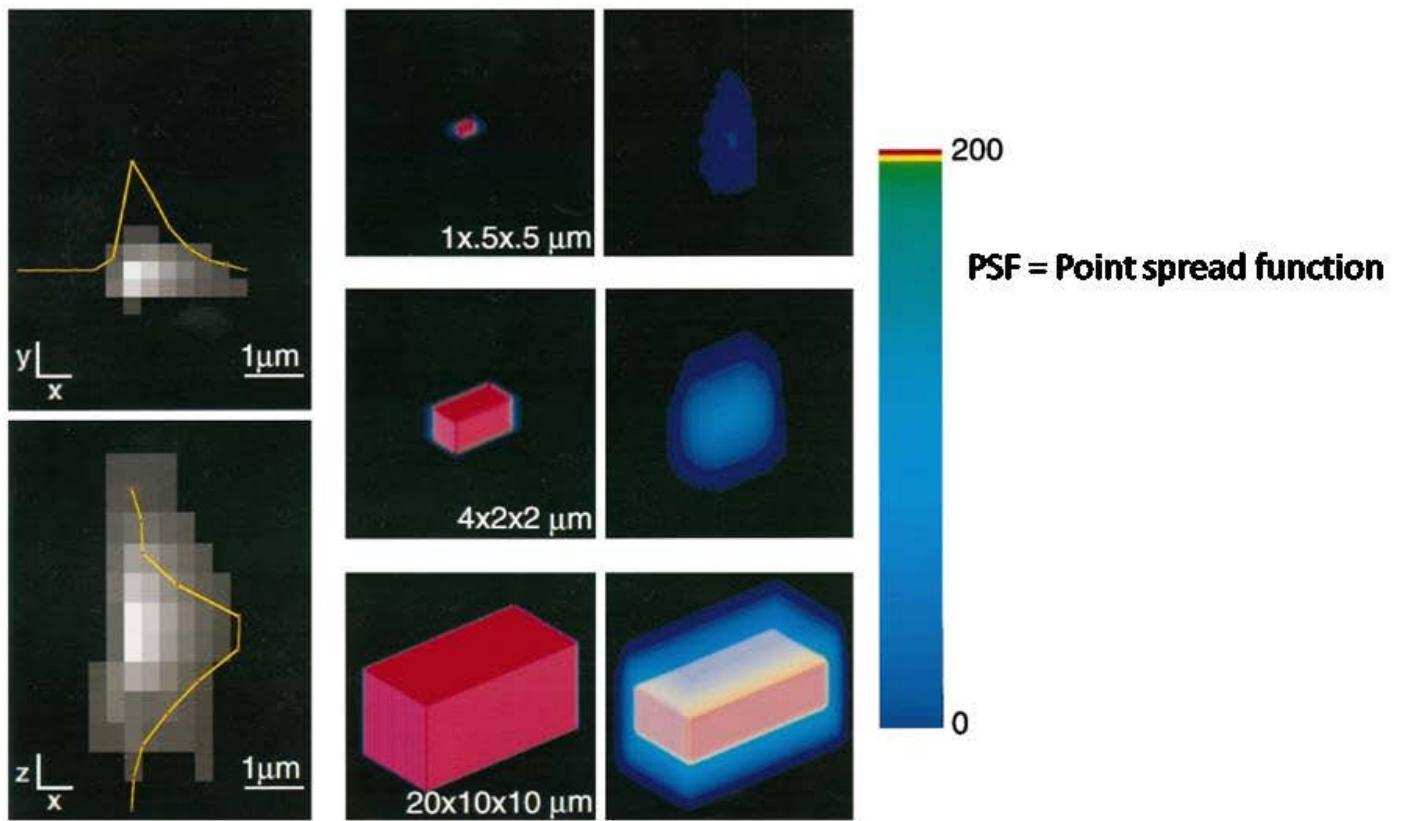
- Easy?/cheap implementation
- Multiscale
- Multicolor



Section 2

Colocalization through Confined Displacement Algorithm CDA

Deconvolución de Imágenes de microscopia confocal



Finky cols. 1998

Problemas de alineación en Microscopia Confocal

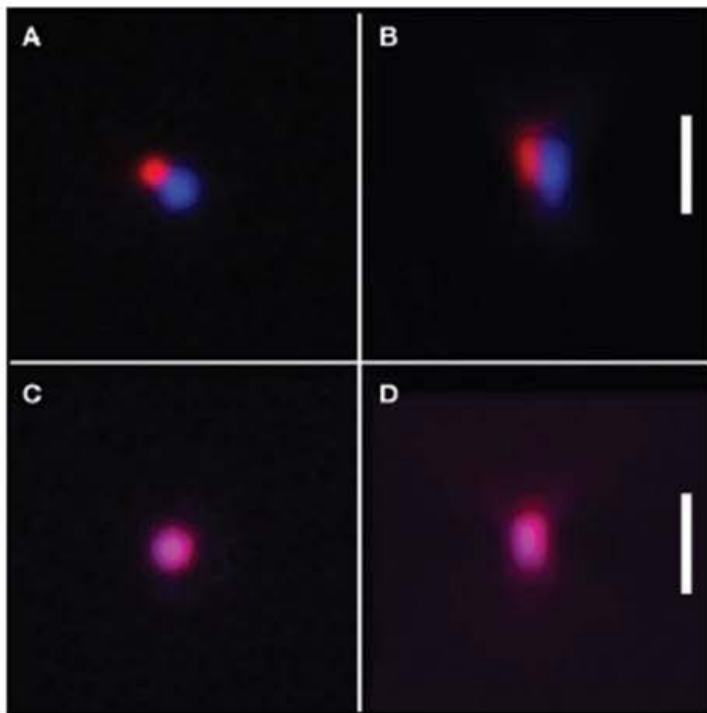
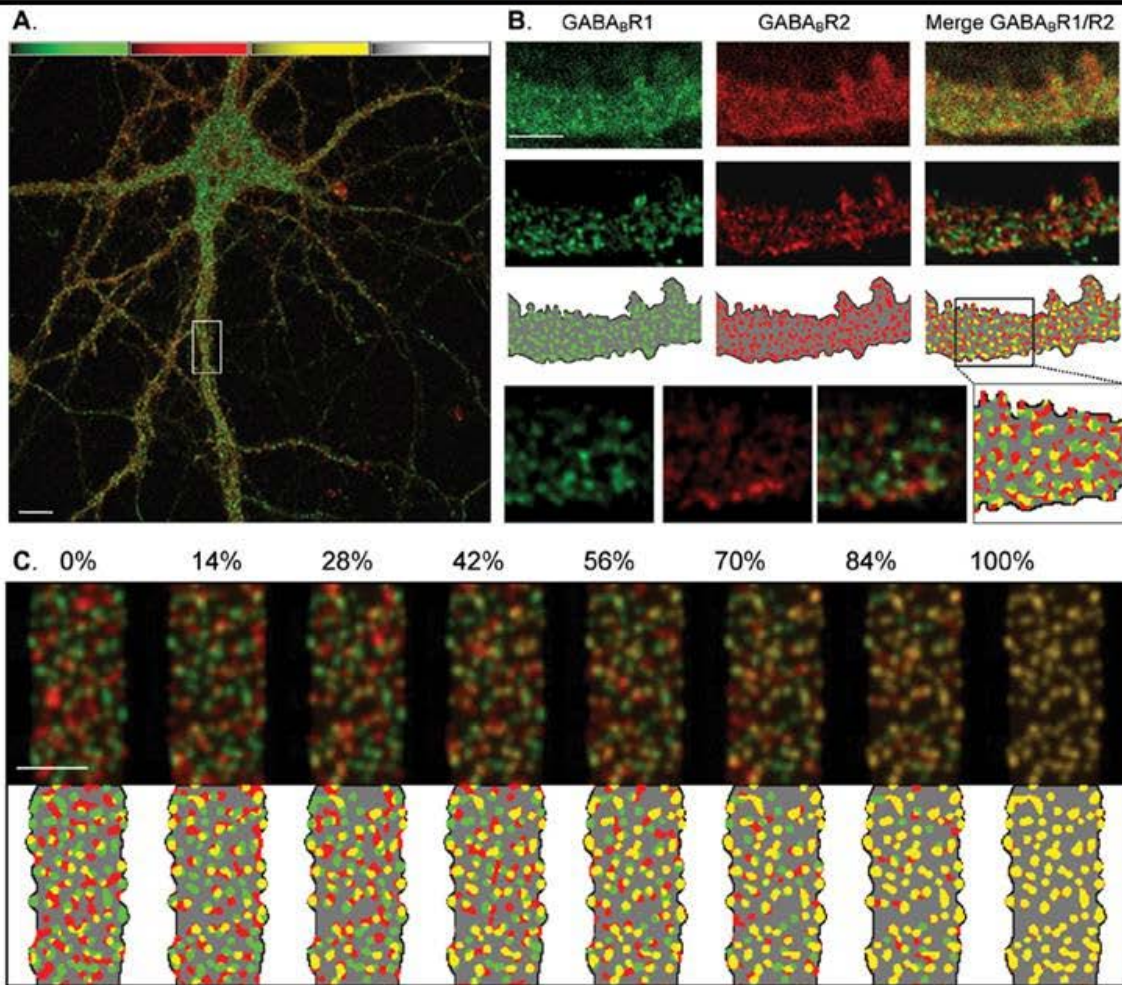


Figure 1. Fluorescent Beads Reveal the Point-Spread Function and Aberrations

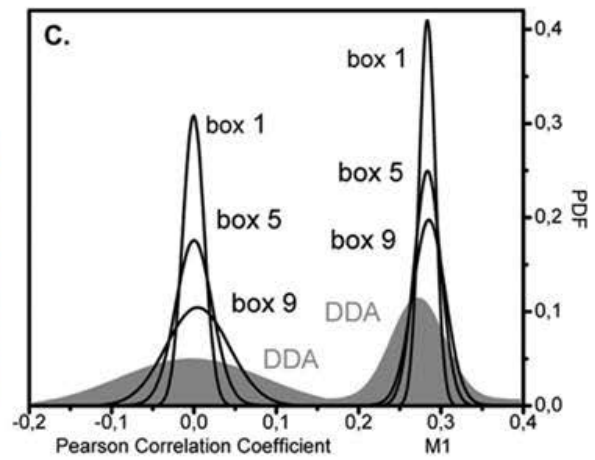
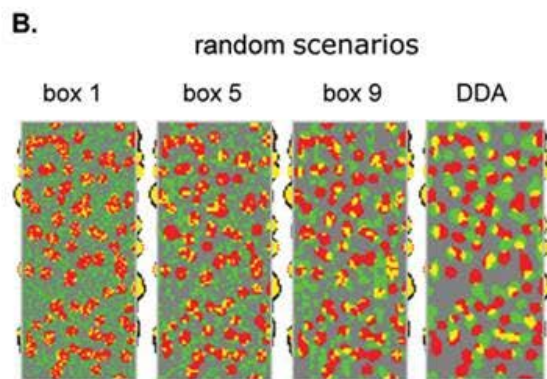
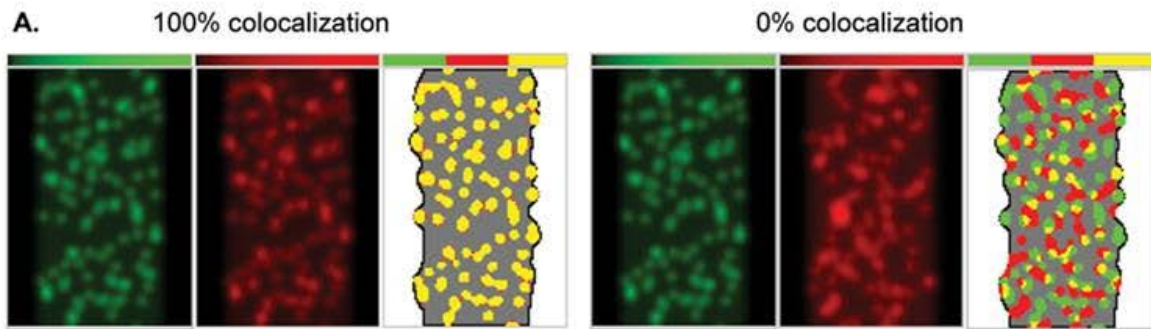
Images of 170 μm spherical beads that fluoresce both blue and red (TetraSpeck beads, Invitrogen/Molecular Probes). Z series images were collected, with both wavelengths collected at each focal plane. (A) and (B) were collected with a PlanApo 100 \times 1.4 NA objective lens. (C) and (D) were taken with a second PlanApo 100 \times 1.4 NA objective lens from the same manufacturer. (A) and (C) are lateral X, Y pseudocolored and overlaid images. In (B) and (D), 3D X, Z reconstructions reveal the axial images, also pseudocolored and overlaid. Note that the axial resolution is worse than the lateral resolution, as is shown by the elongated shape of the spherical bead in Z. (A and B) Lateral axial chromatic aberration in the objective lens causes a shift between wavelengths. (C and D) The second lens has near-negligible chromatic aberration. Comparison of (A) and (B) with (C) and (D) demonstrates the range of aberration correction found in PlanApo lenses. The scale bars represent 1 μm .

Waters y cols. 2008

Discriminación visual de fuentes fluorescentes puntuales en microscopía de fluorescencia

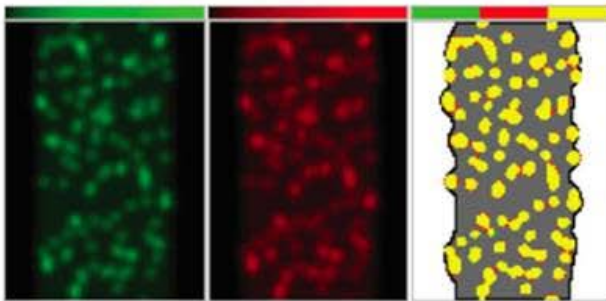


Validación estadística de la colocalización en series de imágenes sintéticas usando el algoritmo de desplazamiento definido

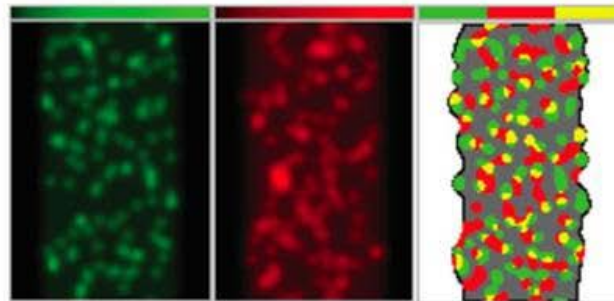


Cálculo de colocalización y CDA

A. 100% colocalization



0% colocalization



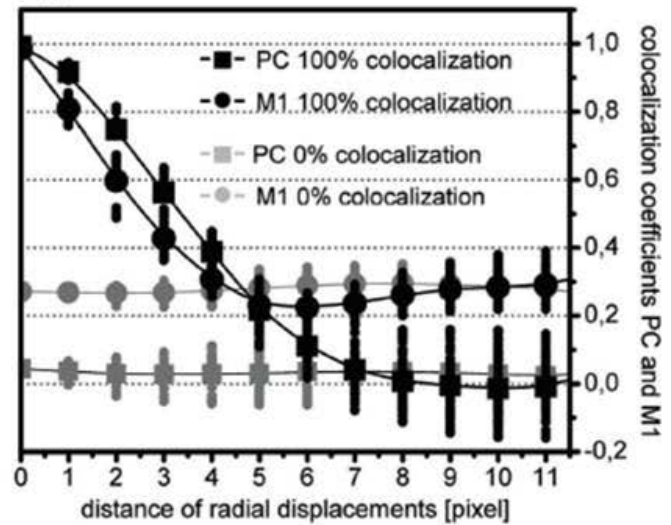
Pearson's coefficient

$$r = \frac{\sum_{i=1}^n ((x_i - \bar{x})(y_i - \bar{y}))}{\sqrt{\sum_{i=1}^n (x_i - \bar{x})^2 \sum_{i=1}^n (y_i - \bar{y})^2}}$$

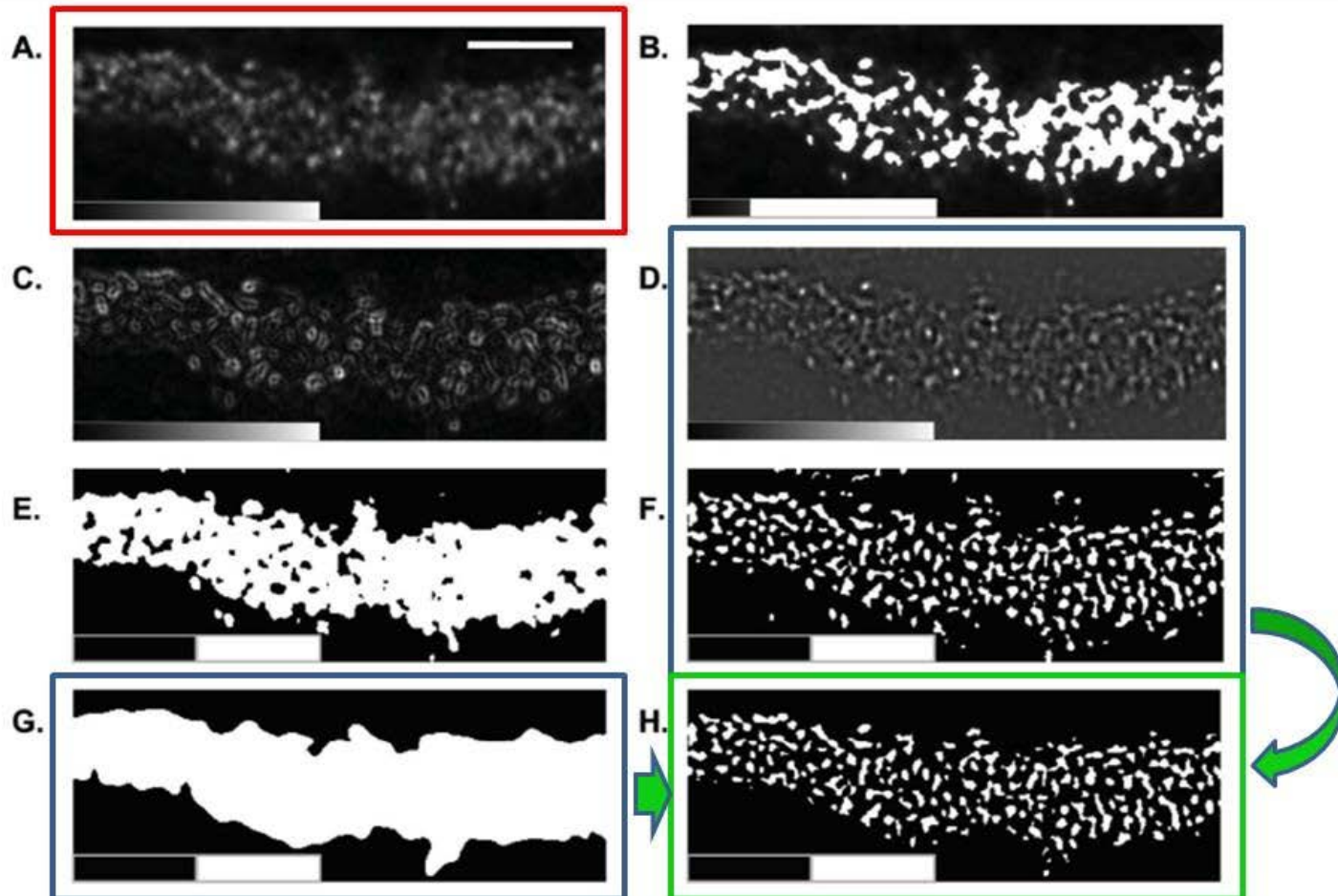
Manders coefficient

$$M_1 = \frac{\sum_i I_{Ch1(ROI1 \cap ROI2)}}{\sum_i I_{Ch1(ROI1)}}, \quad M_2 = \frac{\sum_i I_{Ch2(ROI1 \cap ROI2)}}{\sum_i I_{Ch2(ROI2)}}$$

E.



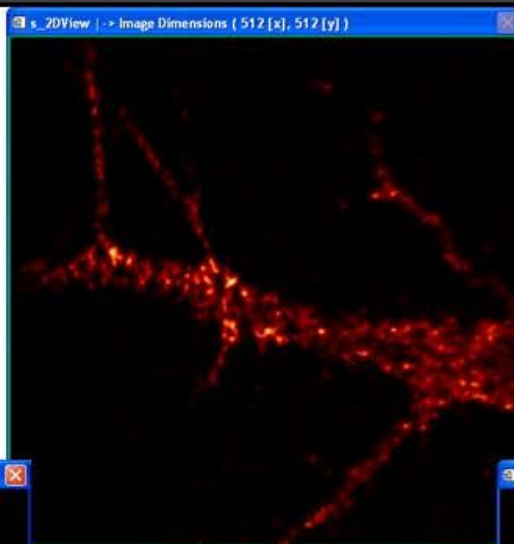
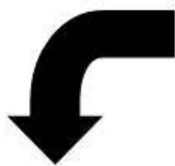
Segmentación de las señales de receptores GABAB en dendritas



Segmentación de las señales de receptores GABAB en dendritas

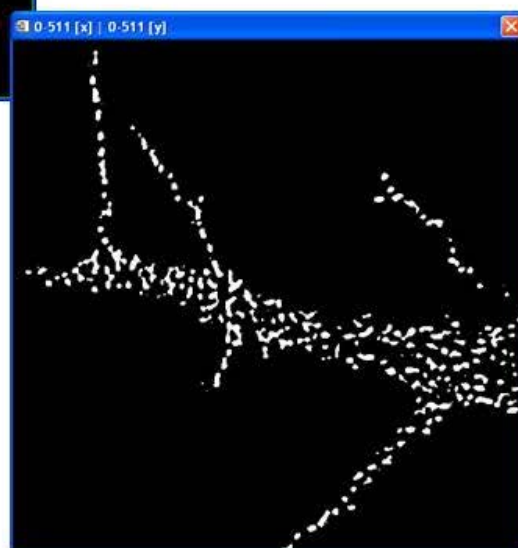
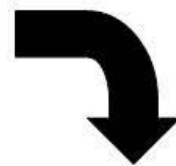
SEGMENTACIÓN

1

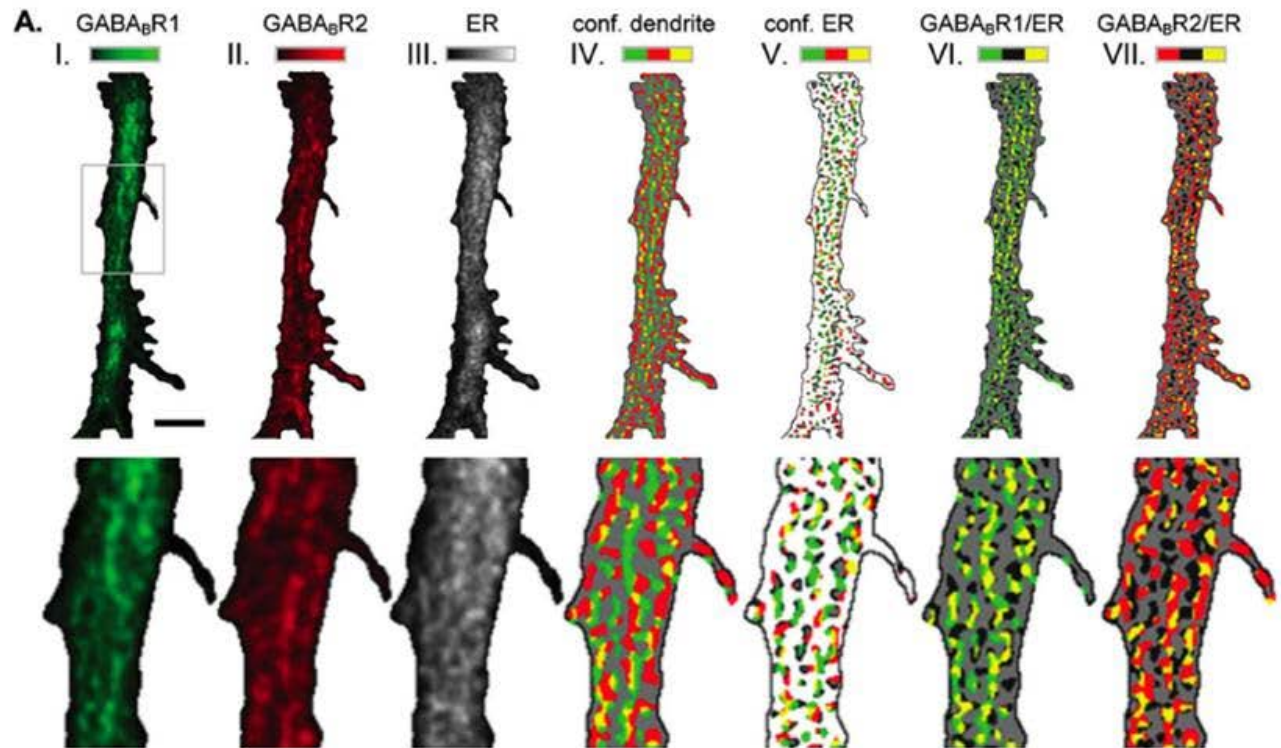


SEGMENTACIÓN

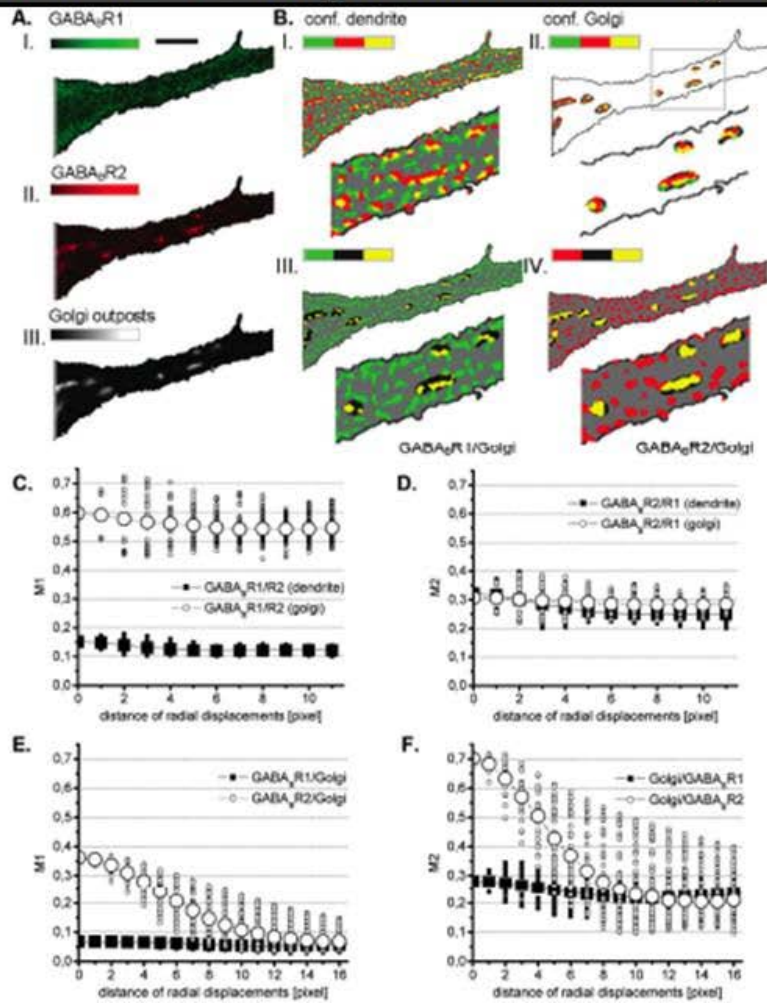
2



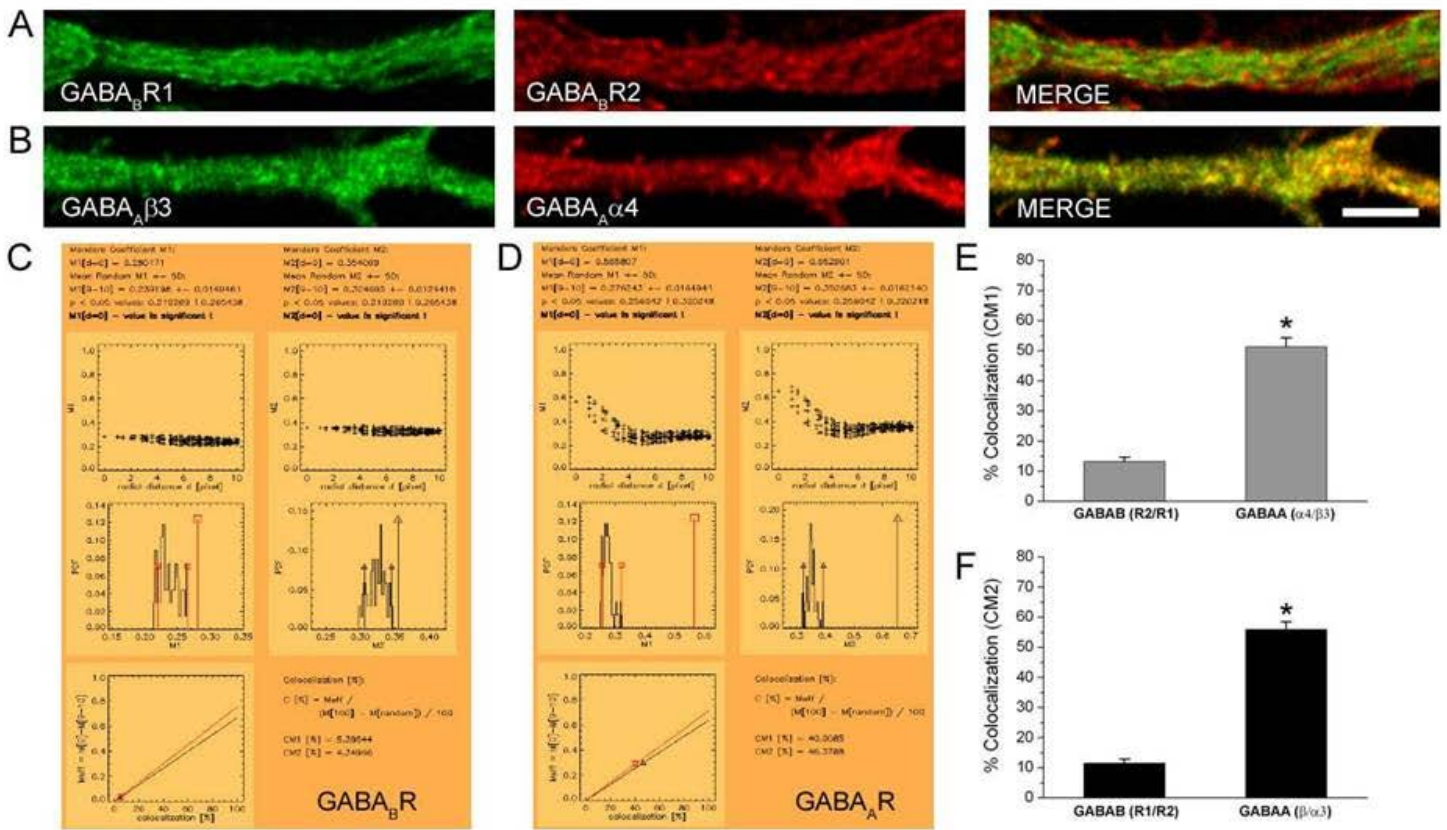
Confinamiento para el cálculo de colocación



CDA revela colocación de GABABR2 con Golgi outposts y colocación aumentada de GABABR1/R2 dentro de los Golgi outposts.



Colocalización de las subunidades de los receptores GABAA comparados con los receptores GABAB: CDA con Manders normalizado



Preguntas?